SECED 2023 Conference
Earthquake Engineering & Dynamics for a Sustainable Future
14-15 September 2023, Cambridge, UK

SHAKE TABLE TESTING ON A FOUR-STORY STEEL FRAME BUILDING WITH SHAPE MEMORY ALLOY CABLE BRACES

Fei SHI[1], Qihao LI[2], Yun ZHOU[3]*, Osman OZBULUT[4]*, & Chao ZHANG[5]

Abstract. *Superelastic shape memory alloys (SMAs) can recover large deformations upon unloading without the need of any external stimuli. Due to their excellent passive re-centering and good energy absorbing capabilities, superelastic SMAs have been considered for various earthquake engineering applications. However, most of the research to date has been on small-scale seismic devices and has remained in proof-of-concept stage. The cable form of SMAs exploits the excellent mechanical properties of thin wires to resist large axial loads. By leveraging the highly optimized manufacturing processes currently available for wires, SMA cables provide a large-capacity structural element with more favorable mechanical properties compared to SMA bars. This study explores the performance of SMA cable bracing systems through shake table tests. SMA cable brace is a promising self-centering system in that it introduces re-centering and energy dissipation through leveraging inherent properties of memory metals, which avoids any fabrication complexities during its assembly, and can easily achieve high force and deformation capabilities by simply varying the cross-sectional area and length of SMA cables. A total of eight SMA cable braces with a load-carrying capacity of 45 kN are fabricated. A four-story steel frame building is designed with the SMA cable braces. Shake table tests on the SMA cable braced steel frame are conducted under various ground motion records and the response of the building is recorded. The results obtained from the shake table test provide a greater understanding on the role of advanced materials and self-centering bracing technologies in achieving an improvement in post-earthquake functionality of building structures and can promote the adoption of these technologies by building owners and communities.*

Introduction

Earthquakes are one of the deadliest types of natural disasters in the world. In addition to claiming countless lives, they can also cause significant damage to infrastructure, resulting in a significant economic loss. Over the past decades, engineers have studied and researched earthquake protection devices in order to improve the seismic resilience of structures, which is the ability to keep occupants safe and minimize damage to the structure during an earthquake. With proper seismic protection devices installed in infrastructure, less lives will be lost, less infrastructure will be damaged, and the economic loss will be less.

Passive dampers are devices such as friction dampers, viscous dampers, and buckling restrained braces that aim to minimize damage to the building to prevent collapse during an earthquake. While they prevent collapse, they do not avoid permanent or residual drift, which would cause the building to have to undergo major repairs or be torn down, resulting in a huge economic loss. Residual drift is how much a building "leans" after a seismic event and it determines the post-event functionality and reparability of structural systems. Passive energy dampers possess many advantages over other types of seismic protection devices, such as their reliability and simplicity. However, many passive energy devices do not have self-centering capabilities, which is important to allow a structure to self-center after a seismic event.

In more recent years, self-centering devices have gained attention for their excellent earthquake resilience and ability to self-center after an earthquake, unlike passive energy dampers. Self-centering devices can minimize residual drifts of a building while provides sufficient energy dissipation energy to control overall response of the building (Zhang et al., 2020). Several self-centering mechanisms such as preloaded disc springs, pre-pressed springs, pre-tensioned

[1] Post-doctoral research associate, Guangzhou University, Guangzhou, China, shifei@gzhu.edu.cn
[2] Graduate Student, Guangzhou University, Guangzhou, China, 2112016180@e.gzhu.edu.cn
[3] Professor, Guangzhou University, Guangzhou, China, zhouyun@gzhu.edu.cn
[4] Associate Professor, University of Virginia, Charlottesville, VA, USA, ozbulut@virginia.edu
[5] Associate Professor, Guangzhou University, Guangzhou, China, zhch2013@gzhu.edu.cn

cables have been studied. Christopoulos et al. (2008) explored a new self-centering energy dissipative bracing system that is able to dissipate energy effectively and self-center within the target design drift. Fang et al. (2021) explored a self-centering device that uses preloaded disc springs working together with friction energy dissipation devices to limit residual drift. Xu et al. (2016) developed and tested a self-centering brace that combines pre-pressed springs and a friction energy dissipation device. Li et al. (2021) explored a new self-centering hybrid damper made of a viscous damper combined with pre-compressed friction springs.

Several researchers have developed shape memory alloy (SMA)-based devices that combine SMAs with various energy dissipating devices. Salehi et al. (2021) explored an SMA-based multi-ring (SBMR) device that uses dampers consisting of superelastic SMA rings and energy dissipating rings. This device can be loaded from multiple directions and installed into a building with a bracing systems. Issa and Alam (2019) explored the new piston-based self-centering bracing system that uses NiTi SMA bars inserted inside a sleeve-piston for the self-centering capability. Wang et al. (2020) explored the mechanical properties and behavior of superelastic SMA angels as a potential new self-centering device. Zhang et al. (2020) explored a new device called a deformation-amplified SMA-friction damper that can be used in reinforced concrete frame structures. Asfaw et al. (2022) fabricated and tested an SMA-based device whose damping capacity is augmented through a frictional energy dissipation. Shi et al. (2023) explored the performance of a SMA-viscoelastic hybrid damper through experimental and numerical studies. Despite the high interest on the development of SMA-based self-centering devices, there is a lack of experimental studies exploring the system level response of buildings with SMA-based devices.

In this study, a self-centering bracing system that relies on unique material properties of superelastic SMA cables is introduced first. Then, a total of eight SMA cable braces are manufactured and the hysteretic behavior of the SMA braces is revealed. Next, a four story steel building is designed with SMA cable braces and shake table tests are conducted. The response of the SMA cable braced frame is studied under various levels of ground motion records.

Shape memory alloy cable braces

The SMA cable utilized in this investigation is made of NiTi alloy in which nickel accounts for 56.06% by weight. The SMA cable is designed with a 7×7×0.885 mm configuration as shown in Figure 1(a). In particular, the SMA cable consists of seven stands wrapped in a right-handed helix, and each strand has seven 0.885 mm diameter wires laid in a left-handed helix. The outer diameter of the formed SMA cables is approximately 8 mm and the cross-sectional area is 30.13 mm^2. Figure 1(b) presents the hysteretic behavior of the SMA cable under increasing loading strain amplitudes from 1% to 6%. It can be observed that the SMA cable possesses good energy dissipation capacity with negligible residual deformation. More information on the mechanical response of SMA cables can be found in Ozbulut et al. (2016) and Shi et al. (2022a).

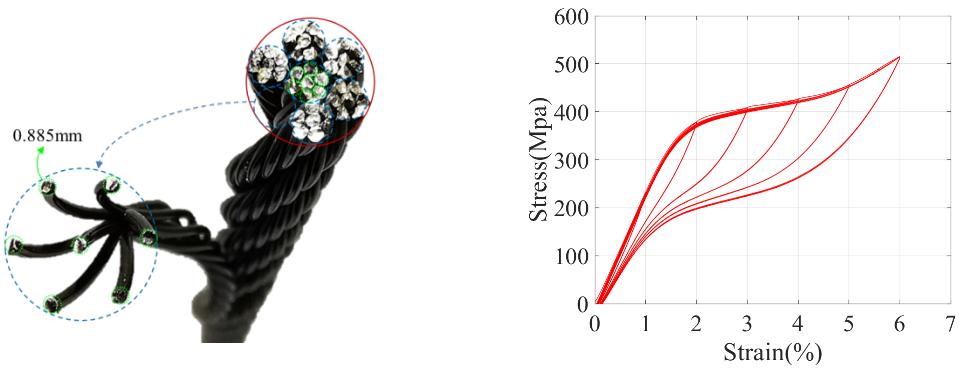

(a) (b)

Figure 1. (a) SMA cable, and (b) hysteretic behavior of SMA cable.

In order to install into a steel frame building for the shake table tests, eight SMA cable bracing systems are designed and manufactured in this study. A schematic view and manufactured specimen of the SMA bracing system are shown in Figure 2(a). The SMA bracing system consists of an outer member, which is a steel box section with a connection plate at one of its end, an inner member, which is a steel I-section with an extended web at one end, two SMA cables, two end plates, a connection plate and two guide members. The inner member is placed into the outer tubular member to guide the SMA cables. The SMA cables are anchored at both ends using a stop end anchorage (Shi et al., 2021) to the end steel plates that can freely move under the guidance of inner member.

The design mechanism of the SMA-based brace enables SMA cables to work in tension when the bracing system itself is either under tension or compression. When the SMA brace is under compression, the inner member moves to the right and pushes the right end plate away. However, the left end plate is blocked by the outer member, which produces tensile forces in the SMA cables. When the bracing system is in tension, the inner member pulls the left end plate but the right end plate is blocked by two guide members attached to the outer box beam (Figure 2(b)). Therefore, the SMA cables again experience tensile loads. This design mechanism enables the SMA cables to be effective whether the brace itself is under tension or compression (Shi et al., 2022b).

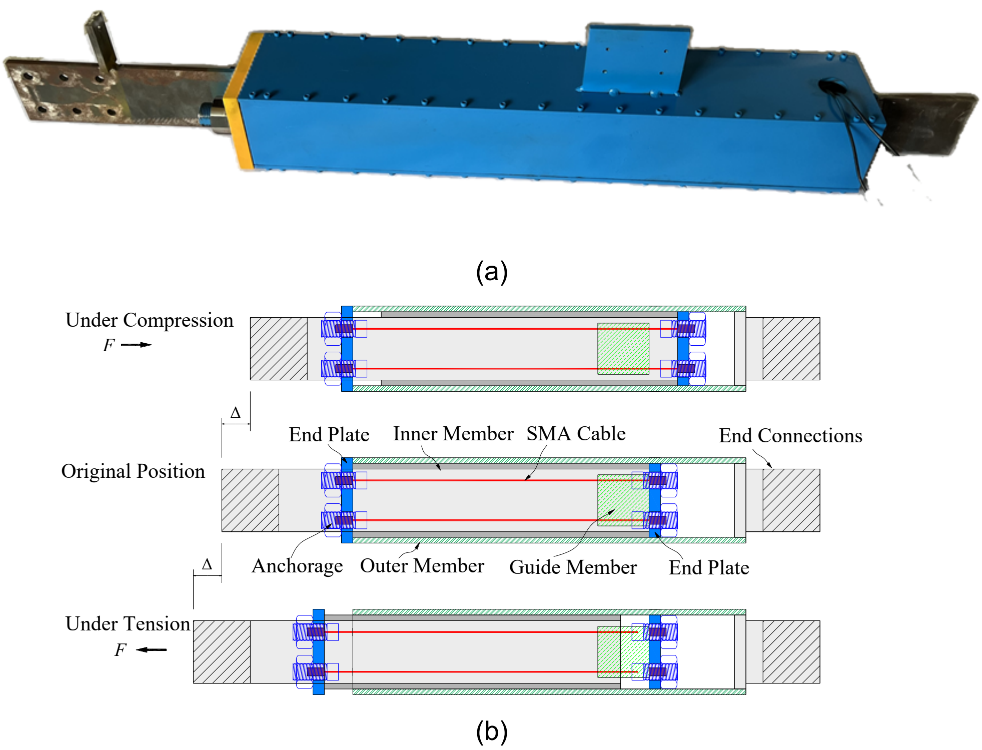

Figure 2. (a) SMA cable brace, and (b) working mechanism of SMA cable brace

An MTS loading frame with 500 kN capacity was employed to conduct a cyclic loading test for the SMA bracing system as shown in Figure 3. The specimen was connected to the MTS setup directly by gripping the connection plates of the SMA brace. The loads were collected by the built-in force transducer of the MTS setup. An additional displacement meter was utilized for measuring the relative deformation between the inner member and outer member of the SMA brace. Note that a pretension of 5 kN is applied to the SMA cables before the test. To enable a stable mechanical behavior of the SMA brace, 30 cycles of cyclic loading at a constant strain amplitude of 6% at 0.01 Hz are conducted for the training purpose.

Figure 3. Test set up.

Figure 4(a) presents the hysteretic response of the SMA brace under 30 cycles of continuous cyclic loading. It can be seen that the curves exhibit strength degradation as the number of loading cycles increases. After the training is completed, the mechanical behavior of the SMA brace is examined with increasing displacement amplitudes from 5 mm to 30 mm. Three cycles of loading are performed at each displacement amplitude. As shown in Figure 4(b), the SMA brace exhibits stable energy dissipation capacity and self-centering ability with high initial stiffness. There is no cyclic strength degradation at any of loading amplitudes.

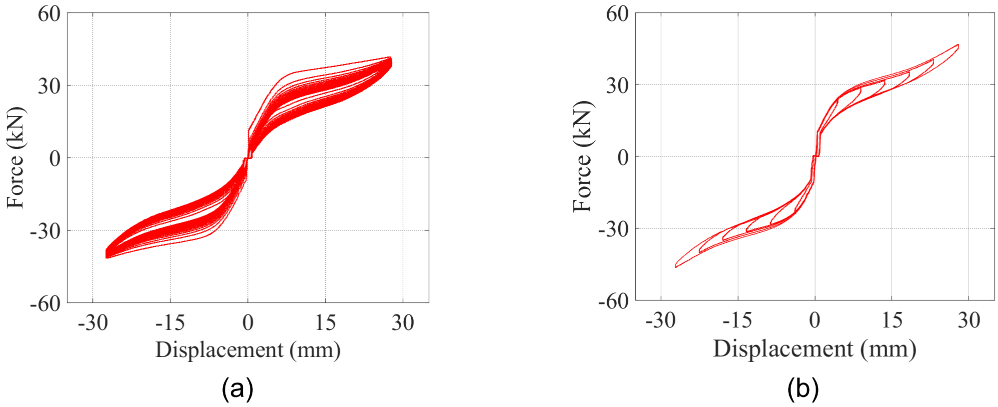

Figure 4. Hysteretic behaviour of SMA brace (a) training loading cycles, and (b) increasing amplitude displacement loading after training

Experimental program

Description of test building

The tested frame is a four-story steel frame building with SMA cable braces. The steel frame building is assumed to be located on soil class II in Shantou City. The building structure is classified as Risk Category C and the design earthquake group is the second group for Shantou City. The frame is designed in accordance with the requirements of Chinese standards. Figure 5(a) shows the plan, elevation view as well as main component dimensions of the tested four-story steel frame building. The steel frame is a semi-rigid frame with SMA bracing system in the W-E direction, which is also the direction of the ground motion input in the test. The SMA cable brace is connected in series with a square steel tube with very high axial stiffness and then diagonally arranged in the semi-rigid steel frame. A total of eight SMA cable braces are installed in the tested frame building. The floor slab is connected to the N-S directional beam only and is used only for the counterweight of the shaking table test.

Figure 5(b) provides the photo of the SMA braced four-story steel frame specimen fixed on a 3 m × 3 m shaking table. The manufactured steel frame has a height of 1.5 m for each story and a span of 2.4 m in the W-E direction. Each floor has an additional weight of 2.2 tons, including 3.2 tons of steel frame, for a total weight of approximately 12 tons. The fundamental period of the tested SMA cable braced steel frame is 0.41s. Displacement sensors and acceleration sensors are arranged on each floor to monitor the seismic response of the steel frame during the test. In addition, a force sensor is mounted in series between the SMA cable brace and square steel tube to measure the force change of the SMA cable brace under ground motion excitation. A displacement meter is also placed on each SMA cable brace to obtain the deformation response during the test.

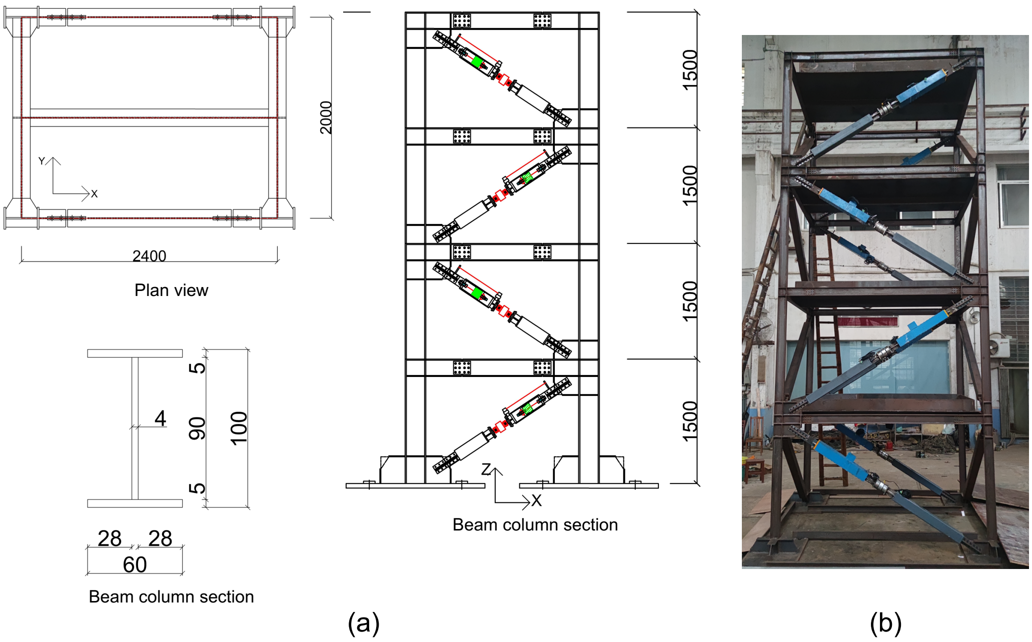

Figure 4. (a) Schematic drawing, and (b) actual photo of the SMA braced steel frame specimen

Ground motion records

A total of three far-field ground motion records are selected for the shake table tests of steel frame with SMA cable bracing systems. The selected far-field ground motions, which are recorded at sites located greater than 55 km from fault rupture, are obtained from the PEER NGA database. The peak ground acceleration (PGA) is used as an intensity measure to scale the individual ground motion records. Figure 6 presents the time history response and the response spectra of individual ground motion records. It can be seen that the response spectra of the selected ground motion records mostly match well with the design response spectrum, while they exhibits high spectral accelerations for periods less than 0.5 s.

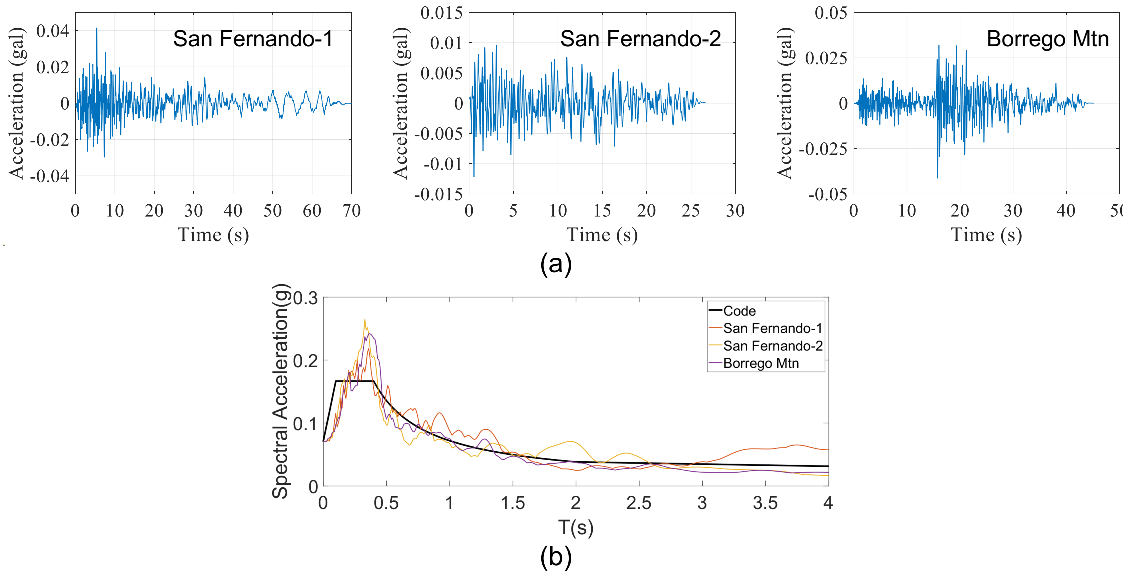

Figure 6. (a) Time history, and (b) response spectrum of selected ground motion record.

Firstly, all three ground motion records scaled to service level earthquake (SLE) hazard level (PGA = 0.07g) are used to excite the SMA cable braced steel frame to examine its seismic performance. Subsequently, the seismic response of the SMA cable braced steel frame under Borrego Mtn record with various intensities is further investigated in terms of interstory drift ratio and hysteretic curve of the SMA cable brace. The PGA of Borrego Mtn record is gradually increased from 0.07g to 0.6g.

Experimental results

Seismic response under various ground motion records

To examine the seismic response of the steel frame with SMA cable braces under the SLE hazard level, the PGA of three far-field ground motions is scaled to a value of 0.07g. After the excitation of the three ground motion records, the displacement response of the steel frame is observed. Figure 7 shows the absolute displacement time history at different stories of the SMA cable braced frame under San Fernando-1 record excitation. It can be seen that the maximum absolute displacement of the steel frame is reaching up to 7.3 mm at the second story. Nevertheless, the maximum absolute displacement and overall vibration response of all four stories are close to each other, indicating that the steel frame is in an elastic state under the SLE hazard level.

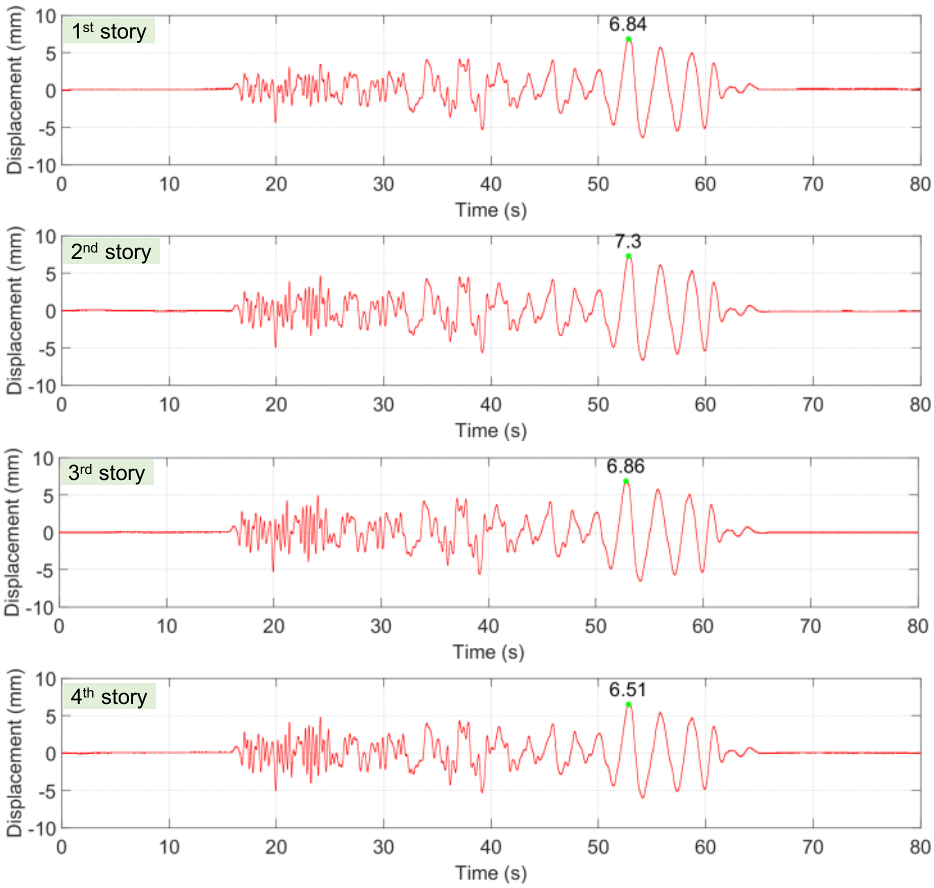

Figure 7. Displacement time history response at different stories of SMA cable braced frame under San Fernando-1 record with PGA of 0.07g.

The interstory drift ratio can be obtained from the difference in the absolute displacement time histories of each story. Figure 8 presents the maximum interstory drift ratio of the SMA cable braced steel frame under all three ground motion records with a PGA of 0.07g. It can be observed that the steel frame subjected to the San Fernando-1 record exhibits the largest interstory drift response. The largest interstory deformation occurs at the first story of the steel frame for all three ground motions under the SLE hazard level. The maximum interstory drift ratio is 0.1%, that is, there is only 1.54 mm interstory deformation. On the other hand, all SMA cable braces are in the elastic deformation phase and contribute only stiffness.

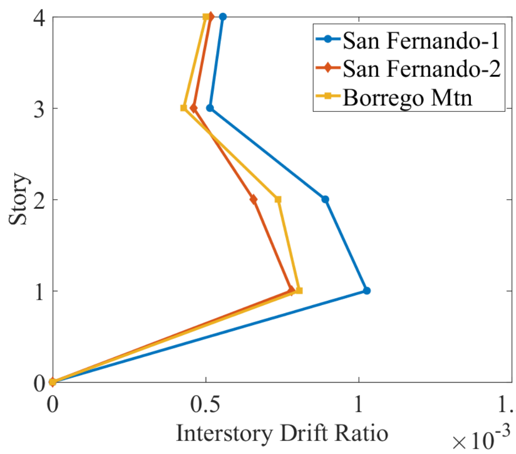

Figure 8. Maximum Interstory drift ratio of SMA cable braced steel frame under various ground motion records with PGA of 0.07g.

Seismic response under increasing ground motion intensities

In order to avoid cumulative damage to the frame, only one ground motion record is selected to further study the seismic performance of the SMA cable braced frame under gradually increasing ground motion intensity. Specifically, the Borrego Mtn record is selected and scaled to PGAs of 0.07g, 0.2g, 0.4g, and 0.6g, corresponding to SLE, design basis earthquake (DBE), maximum considered earthquake (MCE), and extremely rare earthquake hazard levels, respectively, per Chinese code. Figure 9 shows the absolute displacement time history response of the SMA cable braced steel frame under the Borrego Mtn record with increasing intensities. It can be seen that the displacement response of the steel frame increases significantly with the increase of ground motion intensity. The displacement response of high stories is larger than that of low stories. After experiencing a ground motion with 0.6g, the steel frame has negligible residual deformation, indicating an excellent seismic resilience of the steel frame with SMA cable braces.

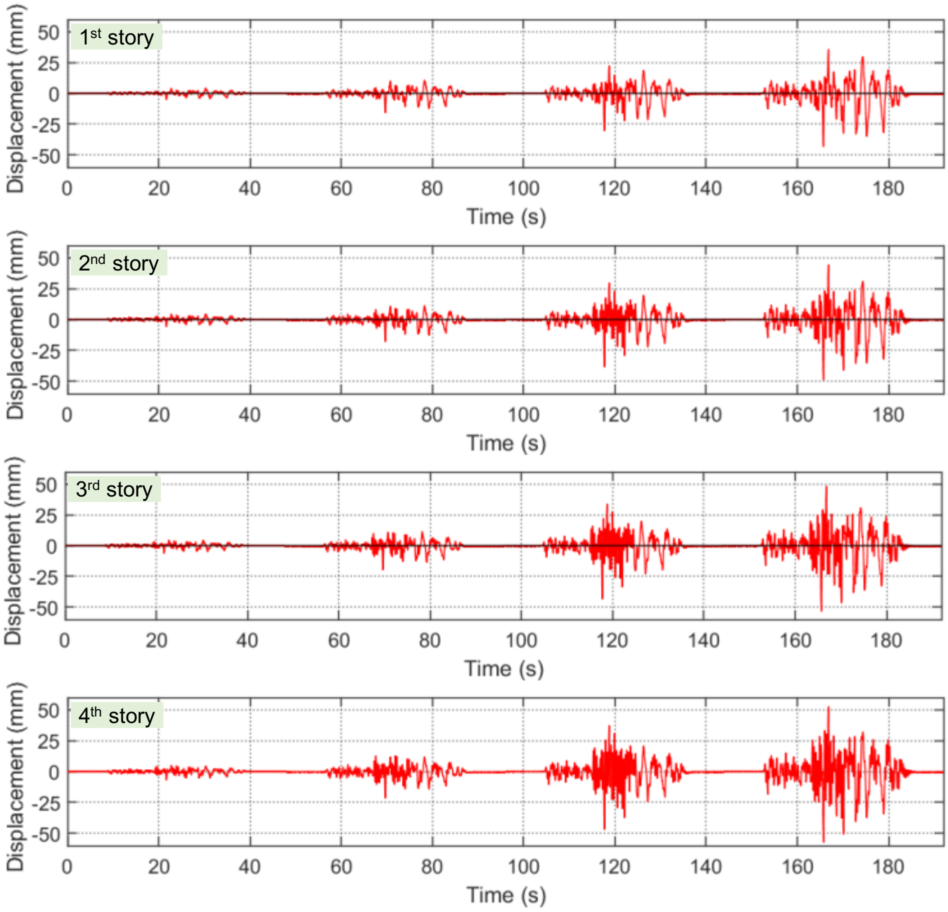

Figure 9. Displacement time history response of SMA cable braced steel frame under Borrego Mtn record with various intensities.

Figure 10 presents the maximum interstory drift ratio for each story of the SMA cable braced steel frame under the Borrego Mtn record with increasing intensity from 0.07g to 0.6g. As expected, the greater the intensity of the input ground motion record, the larger the interstory drift ratio response of the steel frame. As the ground motion intensity increases from 0.07g to 0.6g, the maximum interstory deformation of the steel frame shifts from the first story to the second story. The maximum interstory drift ratios of the steel frame are 0.08%, 0.25%, 0.85%, and 1.04% at intensity of 0.07g, 0.2g, 0.4g, and 0.6g, respectively.

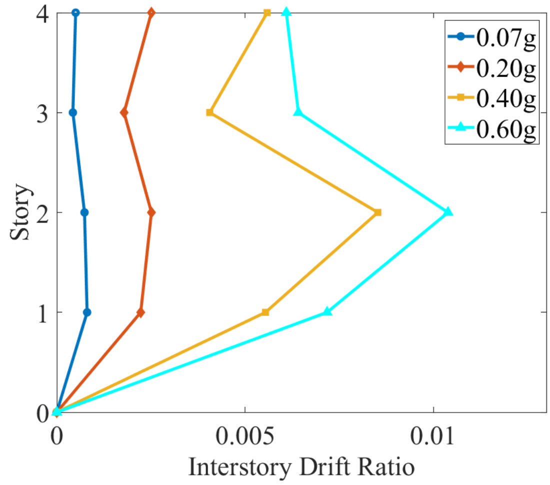

Figure 10. Maximum Interstory drift ratio of SMA cable braced steel frame under Borrego Mtn record with various intensities.

To examine the contribution of the SMA cable braces in the steel frame, the force and displacement of the SMA cable braces are also recorded during the shaking table test. Figure 11 shows a hysteretic response example of two SMA cable braces at the third story under Borrego Mtn record with a PGA of 0.6g. The final moment of the hysteretic response is also highlighted as a red dot in the figure. It can be seen that the two SMA cable braces exhibit typical flag-shaped hysteretic behavior with good energy dissipation capacity and excellent self-centering ability. The maximum displacements of the SMA cable brace I and II reach up to 5.79 mm and 7.19 mm, and the corresponding maximum forces are 24.1 kN and 24.9 kN, respectively. Under the excitation of the Borrego Mtn record, the SMA cable brace I and II at the third story dissipate 502 J and 561 J of energy for the steel frame, respectively. After the seismic excitation is over, the SMA cable braces return to their original position. It can be concluded that the SMA cable braces can effectively dissipate energy and reduce the structural residual deformation to protect the steel frame during an earthquake event, improving the safety and resilience of the steel frame.

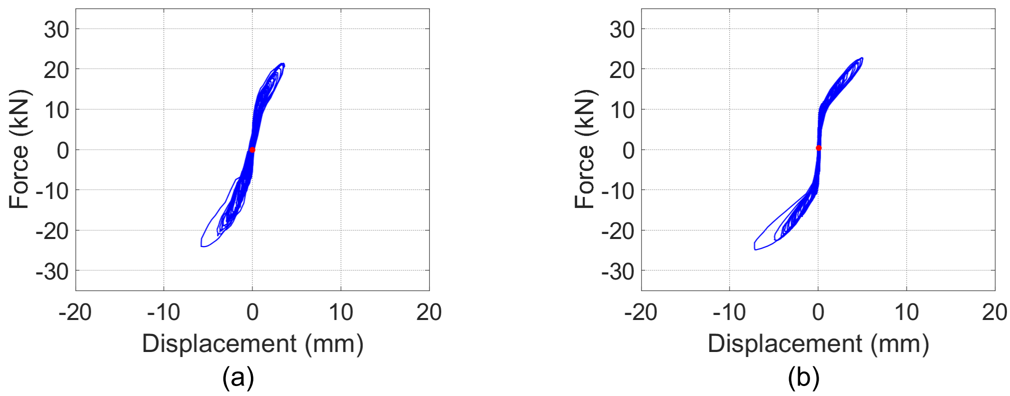

Figure 11. Hysteretic response of SMA cable brace at third story under Borrego Mtn record with PGA of 0.6g: (a) SMA cable brace-I, (b) SMA cable brace-II.

Conclusions

In this study, the seismic response of the SMA cable braced steel frame is investigated through shake table testing. A large-scale SMA cable with a 7×7×0.885 mm configuration is utilized to manufacture a novel self-centering bracing system. Eight SMA cable braces are designed and manufactured for the experiments. A cyclic loading test is conducted to explore the mechanical behavior of the SMA cable brace. The seismic performance of a four-story steel frame incorporating SMA cable braces is experimentally investigated through shaking table tests.

The results from the component testing of the self-centering SMA bracing system indicate that SMA braces has good energy dissipation capacity and excellent self-centering ability, and can easilty be scaled up to large force capacities to meet the actual engineering application requirements. The shake table test results shows the structural response of the steel frame increases considerably with the increase of the input ground motion intensity, however, SMA braces control the response of the system to prevent any excessive story drifts. Benefiting from the contribution of the SMA cable brace in terms of energy dissipation and self-centering ability, the maximum interstory drift of the steel frame under a seismic excitation with PAG of 0.6g reaches only 1.04% with negligible residual deformation.

References:

Asfaw AM, Cao L, Ozbulut OE and Ricles J (2022), Development of a shape memory alloy-based friction damper and its experimental characterization considering rate and temperature effects. *Engineering Structures*, *273*, 115101.

Christopoulos C, Tremblay R, Kim HJ and Lacerte M (2008), Self-centering energy dissipative bracing system for the seismic resistance of structures: development and validation, *Journal of Structural Engineering*, 134(1), 96-107.

Fang C, Wang W and Shen D (2021), Development and experimental study of disc spring–based self-centering devices for seismic resilience. *Journal of Structural Engineering*, 147(7), 04021094.

Issa AS and Alam MS (2019), Experimental and numerical study on the seismic performance of a self-centering bracing system using closed-loop dynamic (CLD) testing, *Engineering Structures*, 195, 144-158.

Li J, Wang W, and Cao Z (2021), Self-centering hybrid dampers for improving seismic resilience, *Engineering Structures*, 244, 112829.

Salehi M, DesRoches R, Hodgson D and Parnell TK (2021), Numerical evaluation of SMA-based multi-ring self-centering damping devices, *Smart Materials and Structures*, 30(10), 105012.

Shi F, Lin Z, Li Q, Ozbulut OE, He Z and Zhou Y. (2023), Design, manufacturing, and testing of a hybrid self-centering brace for seismic resilience of buildings, *Earthquake Engineering & Structural Dynamics*.

Shi F, Zhou Y, Ozbulut OE and Ren F (2022b), Hysteretic response and failure behavior of an SMA cable-based self-centering brace, *Structural Control and Health Monitoring*, *29*(1), p.e2847.

Shi F, Ozbulut OE, Li Z, Wu Z, Ren F and Zhou Y (2022a), Effects of ambient temperature on cyclic response and functional fatigue of shape memory alloy cables, *Journal of Building Engineering*, *52*, p.104340.

Shi F, Zhou Y, Ozbulut OE and Cao S (2021), Development and experimental validation of anchorage systems for shape memory alloy cables, *Engineering Structures*, *228*, p.111611.

Xu LH, Fan XW, and Li ZX (2016), Development and experimental verification of a pre-pressed spring self-centering energy dissipation brace, *Engineering Structures*, 127, 49-61.

Wang B, Zhu S, Chen K, and Huang J (2020). Development of superelastic SMA angles as seismic-resistant self-centering devices, *Engineering Structures*, *218*, 110836.

Zhang Z, Bi K, Hao H, Sheng P, Feng L and Xiao D (2020). Development of a novel deformation-amplified shape memory alloy-friction damper for mitigating seismic responses of RC frame buildings. *Engineering Structures*, *216*, 110751.